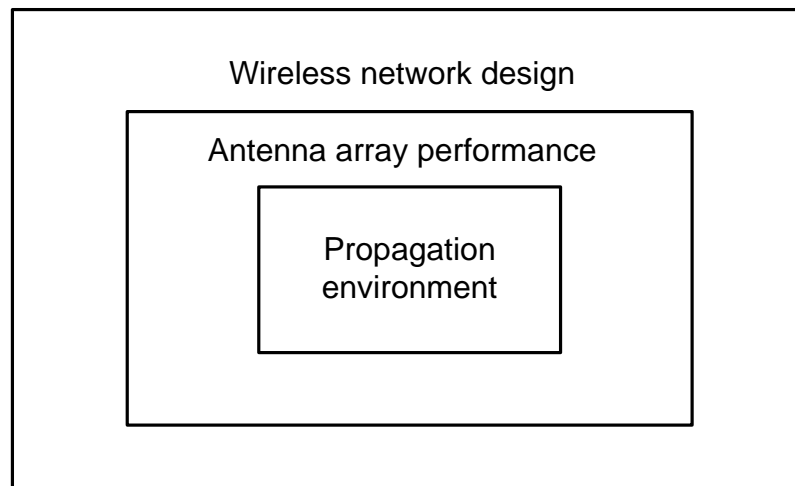


## CHAPTER 2 ANTENNA ARRAYS FUNDAMENTAL

The purpose of this chapter is to present fundamental MIMO antenna array concepts. The performance of antenna arrays is highly dependent upon the propagation environment. Therefore, prior to an evaluation of antenna array performance there must be an understanding of the propagation environment. Figure 2.1 highlights the relationship which exists between network design, antenna array performance, and the propagation environment.



**Figure 2.1** Relationships among wireless network design, antenna array performance, and propagation environment

### 2.1 Linear Diversity Combining Methods

Nowadays, the demand of wireless communication services has been rapidly increasing. It leads the service providers to enhance the capacity of the networks by increasing the number of users without any changes of the existing networks. To reach this purpose, the antenna arrays providing the diversity paths can be advanced to improve the performance of digital cellular radio systems. It can combat the effect of multipath fading of the desired signal and simultaneously reducing the impact of CCI at the receiver [30], [31], [32].

Diversity is a powerful communication receiver technique that provides wireless link improvement at relatively low cost by transmitting many replicas of the same information over independent fading channels to reduce the error occurring at the receiver [33]. In the other words, diversity exploits the random nature of radio propagation by finding independent signal paths for communication. It requires no training overhead since a training sequence is not required by the transmitter. Furthermore, there are a wide range of diversity implementations, many which are very practical and provide significant link improvement with little added cost. In virtually all applications, diversity decisions are made by the receiver, and are unknown to the transmitter. The concept of diversity can be explained simply. If one radio path undergoes a deep fade, another independent path may have a strong signal. By having more than one path to select from, the instantaneous and average SNRs or SINRs at the

receiver may be improved.

There are two types of fading, small-scale and large-scale fading. Small-scale fades are characterized by deep and rapid amplitude fluctuations which occur as the mobile moves over distances of just a few wavelengths. These fades are caused by multiple reflections from the surroundings in the vicinity of the mobile. In order to prevent deep fades from occurring, microscopic diversity techniques can exploit the rapidly changing signal. By selecting the best signal at all times, a receiver can mitigate small-scale fading effects (this is called antenna diversity or space diversity). Large-scale fading is caused by shadowing due to variations in both the terrain profile and the nature of the surroundings. In deeply shadowed conditions, the received signal strength at a mobile can drop well below that of free space. By selecting a base station which is not shadowed when others are, the mobile can improve substantially the average SNR or SINR on the forward link. This is called macroscopic diversity, since the mobile is taking advantage of large separations between the serving base stations. Macroscopic diversity is also useful at the base station receiver. By using base station antennas that are sufficiently separated in space, the base station is able to improve the reverse link by selecting the antenna with the strongest signal from the mobile.

In recent years, space diversity with antenna arrays that are at least a half of a wavelength apart has been considerably interested due to its ability to mitigate the effect of multipath fading and cochannel interference, and thus allows digital cellular radio systems to operate effectively in high interference environments. With  $N$  antenna arrays, the  $N - 1$  interferers can be negligible [34]. Therefore, this technique can be an alternative in improving the capacity of the existing networks instead of using cell splitting or microcells that can preface handoff problems and more complexity in planning new base stations and frequency reuse. By using antenna arrays, the complexity of the network controller can be reduced and it is also less expensive than using microcells. Additionally, the low power transmitters can be operated with high power transmitters without degrading the system performance [34].

### 2.1.1 Practical Antenna Diversity

Antenna or space diversity is one of the most popular forms of diversity used in wireless systems. Conventional wireless systems consist of an elevated base station antenna and a mobile antenna close to the ground. The existence of a direct path between the transmitter and the receiver is not guaranteed and the possibility of a number of scatterers in the vicinity of the mobile suggests a Rayleigh fading signal [35].

The concept of antenna diversity is also used in base station design. At each cell site, multiple base station receiving antennas are used to provide diversity reception. However, since the important scatterers are generally on the ground in the vicinity of the mobile, the base station antennas must be spaced considerably far apart to achieve decorrelation. Separations on the order of several tens of wavelengths are required at the base station. Space diversity can thus be used at either the mobile or base station, or both. Figure 2.2 shows a general block diagram of a space diversity scheme [36]. Space diversity methods can be classified into five main categories as follow [37].

#### a) Selection Diversity

Selection diversity is the simplest diversity technique. A block diagram of this method is similar to that shown in Figure 2.2, where  $M$  demodulators are used to provide  $M$

diversity branches whose gains are adjusted to provide the same average SNR or SINR for each branch. The receiver branch having the highest instantaneous SNR or SINR is connected to the demodulator. The antenna signals themselves could be sampled and the best one sent to a single demodulator. A practical selection diversity system cannot function on a truly instantaneous basis, but must be designed.

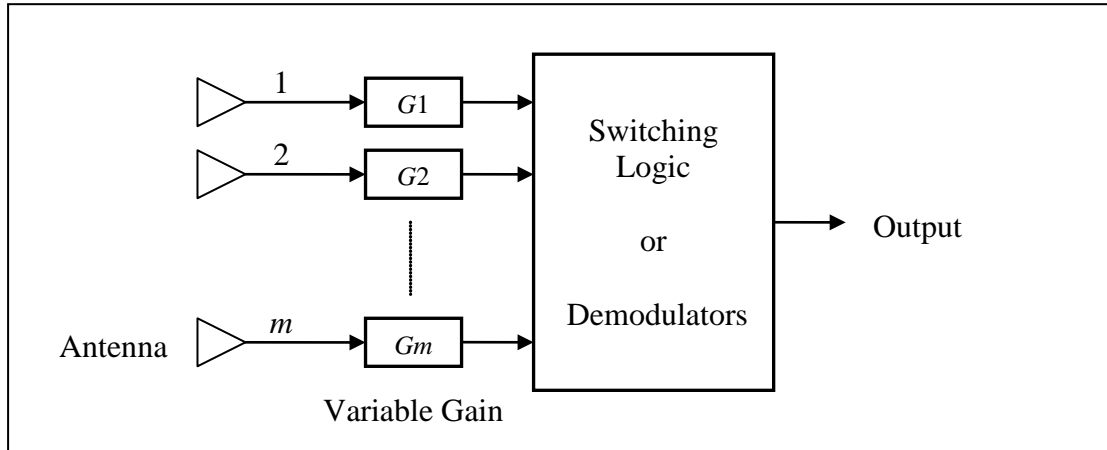


**Figure 2.2** Generalized block diagram for space diversity [38]

#### b) Feedback Diversity

Feedback diversity is very similar to selection diversity except that the  $M$  signals are scanned in a fixed sequence until one is found to be above a predetermined threshold, instead of always using the best of  $M$  signals. This signal is then received until it falls below threshold and the scanning process is again initiated. The resulting fading statistics are somewhat inferior to those obtained by the other methods, but the advantage with this method is that it is very simple to implement, only one receiver is required. A block diagram of this method is shown in Figure 2.3.

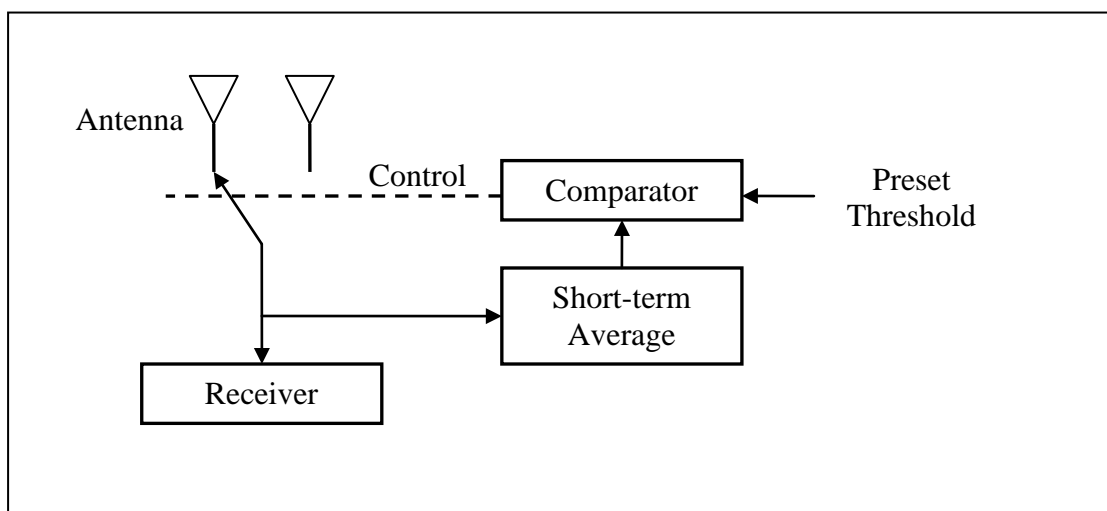


**Figure 2.3** Basic form of scanning diversity [38]

### c) Maximal Ratio Combining

In this method, the signals from all of the  $M$  branches are weighted according to their individual signal voltage to noise power ratios and then summed as shown in Figure 2.4. The individual signals must be co-phased before being summed, unlike the selection diversity, which generally requires an individual receiver and phasing circuit for each antenna element. Maximal ratio combining produces an output SNR or SINR equal to the sum of the individual SNRs or SINRs. Thus, it has the advantage of producing an output with an acceptable SNR or SINR even when none of the individual signals are themselves acceptable. This technique gives the best statistical reduction of fading of any known linear diversity combiner so that this optimal form of diversity is now practical.

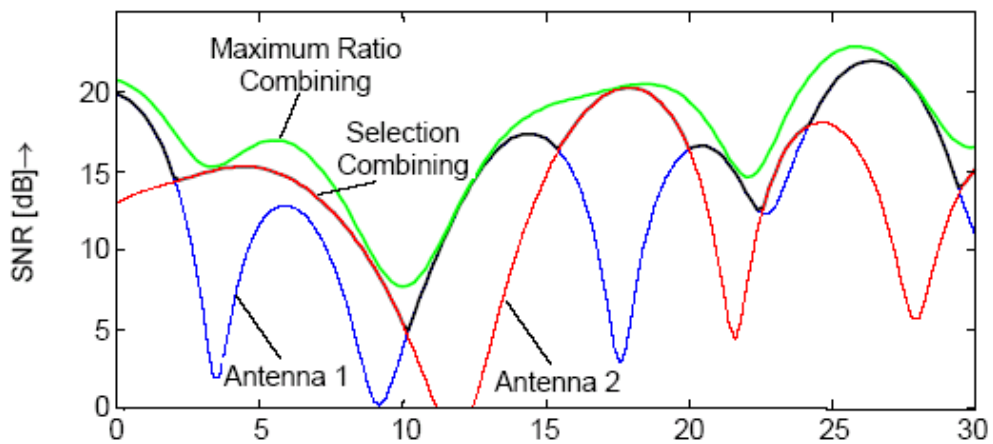


**Figure 2.4** Comparison of diversity receivers MRC and SC

### d) Equal Gain Combining

In certain cases, it is not convenient to provide for the variable weighting capability required for true maximal ratio combining. In such cases, the branch weights are all set to unity, but the signals from each branch are co-phased to provide equal gain combining diversity. This allows the receiver to exploit signals that are simultaneously received on each branch. The possibility of producing an acceptable signal from a number of unacceptable inputs is still retained, and performance is only marginally inferior to maximal ratio combining and superior to selection diversity.

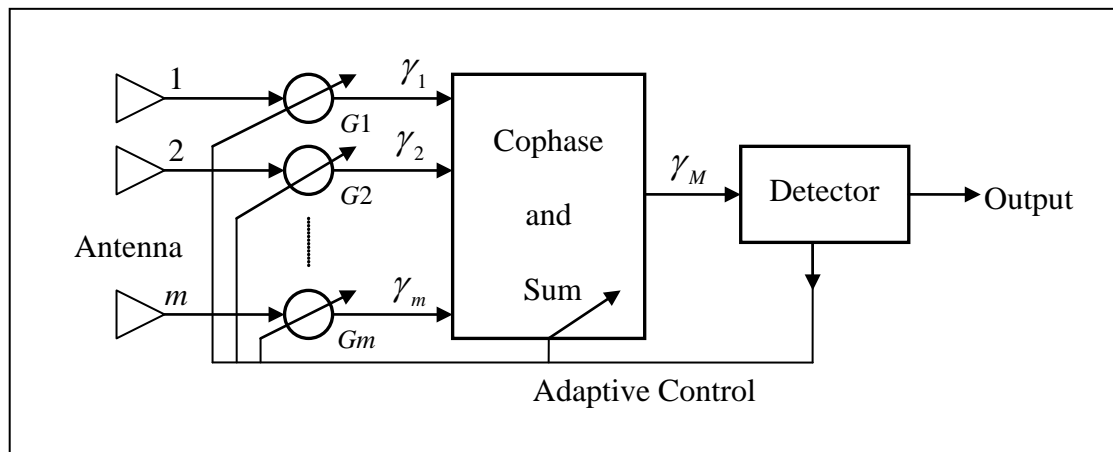


**Figure 2.5** Maximal ratio combiner [38]

### e) Optimum Combining

In optimum combining or Minimum Mean Squared Error method, all antenna channels in a system keep the gain and phase under control as in maximal ratio combining method and it can also include the equal gain combining method as a special cases. The signals received by several antenna elements can be properly weighted and combined to maximize the output SNR or SINR [39].

The implementation of this method requires channel estimation for the desired signal as well as for all the interfering signals. Even the implementation and performance analysis of systems employing this method are quite complicated, it gives the best performance and can be substantial in more fading environments [39], [40]. Therefore, optimum combining is the main focus of this research in investigating the performance of a system employing diversity reception in the presence of non-Gaussian multipath fading channel.

## 2.2 Previous Work

The performance of digital cellular systems over fading channels, in presence of interference and noise is measured by outage probability [2]-[7]. In order to calculate the outage probability, it is necessary to know the probability density function (pdf) of the desired and interfering signals. It has been well known that the Gaussian process is widely used to model multipath fading channel due to assumption of central limit theorem (CLT). In practical, however, there exist many environments such that the CLT cannot be applied and the Gaussian process is invalid or fails to describe the phenomenon of wave propagation [8]. In addition, only one or two co-channel interferers dominate the signal disturbance of most users in narrowband cellular systems such as GSM. In this case, the Gaussian model does not accurately represent the statistics of co-channel interference [9]. Therefore the statistical property of multipath fading is characterized as a non-Gaussian process. Thus far, the capacity analysis of MIMO systems has primarily focused upon Rayleigh and Rician fading channels, e.g., [13-14] and the references therein. However, the capacity results for MIMO non-Gaussian fading channels are much limited.

Initially SIMO systems rely on the use of  $n \geq 2$  antennas at the receiver to achieve diversity. If these multiple antennas are sufficiently spaced, one might expect that the different diversity branches fade independently, provided that the physical channel shows favorable properties. However, analytical and computation results in many literatures show that the SIMO systems performance is lower than MIMO systems.

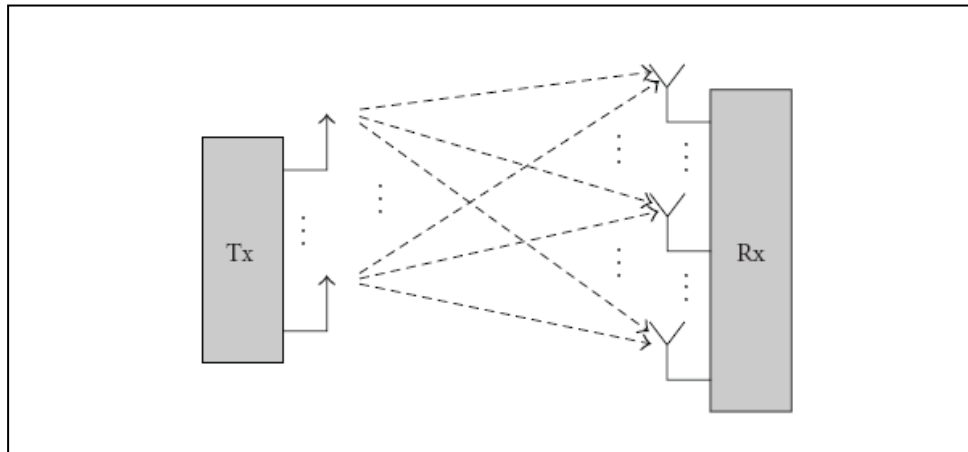


**Figure 2.6** Schematic illustration of a MIMO system with multiple transmits and receives antennas

In Figure 2.6, the pioneering work of [15-16] has contributed to highlight the potential of multi-antenna systems in allowing for higher data rates to be efficiently conveyed over wireless fading channels. MIMO MRC have already been considered and shown to provide Rician fading and Rayleigh fading channels [17-18]. The Khatri distribution of the largest eigenvalue of central complex Wishart matrices is investigated. Model of indoor and outdoor MIMO channel have been reported in [19-20], respectively. The effects of non-identical fading distribution on the performance of space time modulation are addressed in [21]. However, SNR is only considered. The MIMO based on antenna selection was developed by M. Ramezani, et al. [22], with this selection method, Rician fading channels between the Tx-Rx antennas is considered.

Because of their great promise, MIMO is also being considered but not finalized. In a MIMO system employing OC scheme in presence of co-channel interference studied in [23], the system performance in term of outage probability in Rayleigh fading scenarios. In [24] the authors derived a closed form expression for the MIMO-OC in correlated Rayleigh fading channels. Based on Gaussian random matrices and signal to interference ratio (SIR) are investigated in interference limited environment without noise. Since the most previous work, other fading characteristics have been considered as for Rician and Rayleigh case. A more realistic MIMO-OC non-Gaussian channel has not been addressed.

### 2.3 Central Limit Theorem

To understand the propagation of multipath fading channel, the input signal at a receiver is usually written as a sum of finite  $K$  random vectors as

$$R e^{j\theta} = \sum_{k=1}^K A_k e^{j\varphi_k} = X_C + X_S \quad (2.1)$$

where there is  $K$  vectors with corresponding amplitude  $A_k$  and phase  $\varphi_k$ . The variable  $R$  and  $\theta$  are respectively the resultant envelope and phase of the received signal with the random amplitudes  $A_k$  and phases  $\varphi_k$ . The variable  $X_C$  and  $X_S$  are respectively the in-phase and quadrature-phase components of the resultant vector.

When  $K$  is large enough, the received signal may be modeled by Gaussian process due to the central limit theorem (CLT) assumption. Due to practical consideration and mathematical tractability, this classical Gaussian model has been widely used to model the multipath fading process and the cochannel interference process. The Gaussian assumption for the in-phase and quadrature-phase components of the received random vectors leads to the commonly used Rayleigh and Rice envelope distributions and uniform phase distribution.

In practice, the CLT assumption which lies beneath the usual Gaussian approximation is not always valid to describe the phenomenon of wave propagation [41], [42]. It may not generally be appropriated under any of the following three conditions, which are frequently occurred in many mobile communication environments.

- The number of terms  $K$  is not sufficiently large for the CLT to hold. Therefore, the sum of quadrature components, i.e.  $X_C$  and  $X_S$ , is not Gaussian distributed. However, some justifications had been considered for the rapidity of convergence of the sum in (3.1) to a Gaussian process and the appropriateness of the magnitude of  $K$  for CLT assumption when the process is zero-mean [41], [42].
- The number of terms  $K$  is itself random. When  $K$  is not constant, the distribution of the sum is not appropriate to be approximated by a Gaussian process, except for some specific cases. Particularly, when the number of vectors  $K$  is random, it can be shown that the CLT holds if elementary phase is uniformly distributed and the condition that  $\sqrt{(E[K^2])/E[K]^2) - 1} \rightarrow 0$  is satisfied [41], [42].
- The condition that  $E[A_k^2] \ll E[R^2]$  is unsatisfied for some values of  $k$ . In this case all terms of those  $k$  will dominate the others and the pdf of sum will be determined by those pdfs.

With the conditions mentioned above, the assumption of normality may not be satisfied and the resulting process becomes a non-Gaussian random process. A new kind of multipath fading model, which is not based on the Gaussian assumption, is desirable. This model can yield the multivariate non-Gaussian pdf when there is correlation between samples and it can provide mathematical tractability as well.

Many practical problems involve the probability density function (pdf) of the envelope of the sum of a sinusoidal signal and noise. this random signal is also used to model the multipath fading channel and can be considered as random vectors with random amplitude and phase as in (2.2) [41]. The variable  $X_C$  and  $X_S$  that are the in-phase and quadrature-phase components of the resultant vector, respectively, can be written as

$$X_C = \sum_{k=1}^K A_k \cos \varphi_k \quad (2.2)$$

$$X_S = \sum_{k=1}^K A_k \sin \varphi_k \quad (2.3)$$

Therefore, the envelope and phase of the received signal can be written as

$$R = \sqrt{X_C^2 + X_S^2} \quad (2.4)$$

$$\theta = \tan^{-1} \left( \frac{X_S}{X_C} \right) \quad (2.5)$$

The statistical properties of the multipath fading channel can be completely characterized by the knowledge of the joint pdfs of random variables  $R$  and  $\theta$ . Two models that are commonly used are the Rayleigh and Rice envelope distributions. Both statistical models are based on the assumption of a sufficiently large number ( $K$ ) of random vectors and uniformly distributed phase for each individual vector. Therefore, the central limit theorem (CLT) can be applied and the corresponding  $X_C$  and  $X_S$  are characterized by a joint Gaussian distribution. However, there are several conditions under which the CLT may not hold in practice as mentioned above. As a result of any of these reasons, when the CLT is not valid, the components  $X_C$  and  $X_S$  are jointly non-Gaussian distributed random variables. Thus, the pdf of the resultant envelope  $R$  is no longer Rayleigh or Rice distributed.

As mentioned in [41], the joint pdf of the non-Gaussian quadrature components was obtained by a series expansion in terms of Hermite polynomials, and the corresponding non-Rayleigh envelope pdf derivation. The non-Gaussian quadratures have also been modeled as spherically invariant random processes (SIRP) [43], [44], [45]. The system performance has also been decomposed in the complex non-Gaussian channel into the sum of two terms, namely, one attributed to the usual Gaussian quadratures plus a residual term that is expressed as a series in terms of multidimensional Hermite polynomials whose coefficients are the channel quasi-moments [46], [47]. Moreover, non-Gaussian quadrature components have also been considered for the case when the number of random vectors  $K$  is a random variable [41], [48], [49] as well as for the case of non-uniformly distributed phase  $\varphi_k$  [41], [50]. As none of the exact envelope pdfs when the quadrature components are non-Gaussian distributed are derived in closed form, the envelope pdfs are usually approximated in terms of infinite series expansion in Hermite polynomials or in terms of numerical integration and the Rayleigh or Rice distributions obtained as special cases. Therefore, it is attractive to derive the closed-form expression for the envelope distribution when the quadrature components are non-Gaussian distributed.

## 2.4 Analytical Consideration

In digital cellular radio communication systems, the channel is generally conducted to multipath fading and the system performance is degraded by the cochannel interference. In this study, the system that includes an  $M$ -element antenna array at the receiver is considered operating in the presence of  $N$  cochannel interferers. The associated linear diversity combiner is expressed mathematically using a complex notation [51]. The signals received at the output of an  $M$ -element antenna array operating in the presence of  $N$  interferers can be written as

$$\mathbf{r}(t) = s_0(t) \cdot \mathbf{A}_0 + \sum_{i=1}^N s_i(t) \cdot \mathbf{A}_i + \mathbf{n} \quad (2.6)$$

where  $s_i(t)$  ( $i=0,1,2,\dots,N$ ) are the transmitted signals,  $\mathbf{A}_i$  ( $i=0,1,2,\dots,N$ ) are the  $M$ -dimensional direction of arrivals of the desired signal ( $i=0$ ) and the interfering signals ( $i=1,2,3,\dots,N$ ), respectively. According to the representation theorem of SIRP [71], the vector  $\mathbf{A}_i$  can be written as the product of a non-negative random variable  $u_i$  and a zero-mean complex Gaussian random vector  $\mathbf{Z}_i$ .

$$\mathbf{A}_i = u_i \mathbf{Z}_i \quad (2.7)$$

where  $u_i$  and  $\mathbf{Z}_i$  are assumed to be independent for  $i=0,1,2,\dots,N$ . The vectors  $\mathbf{Z}_i$  ( $i=1,2,3,\dots,N$ ) are also assumed to be independent, identically distributed (iid) and zero-mean complex Gaussian random vectors.

For further assumption, each component of the vectors  $\mathbf{A}_i$  is a complex spherically invariant random vector with mean power of  $P_i$  ( $i=0,1,2,\dots,N$ ). The vector  $\mathbf{n}$  is an additive Gaussian noise vector with zero mean and covariance matrix  $\sigma_n^2 \mathbf{I}$ , where  $\sigma_n^2$  is the noise power or the covariance of each element in  $\mathbf{n}$  and  $\mathbf{I}$  is an  $M \times M$  identity matrix. The covariance matrix is given by [39]

$$\mathbf{R} = E \left[ \left( \sum_{i=1}^N \mathbf{A}_i \mathbf{A}_i^H + \mathbf{n} \right)^H \left( \sum_{i=1}^N \mathbf{A}_i \mathbf{A}_i^H + \mathbf{n} \right) \right] \quad (2.8)$$

where the superscript  $H$  denotes the Hermitian transpose of the complex vector. The expected value in (2.8) is taken over a period much less than the reciprocal of the modulated symbol duration, assuming that the fading rate is much slower than the bit rate of the transmitted signal. Assuming that all interferences and noise are uncorrelated, the covariance matrix  $\mathbf{R}$  can be written as

$$\mathbf{R} = \sum_{i=1}^N \mathbf{A}_i \mathbf{A}_i^H + \sigma_n^2 \mathbf{I} \quad (2.9)$$

where  $\mathbf{A}_i$  ( $i=0,1,2,\dots,N$ ) are the  $M$ -dimensional direction of arrivals of the desired signal ( $i=0$ ) and the interfering signals ( $i=1,2,3,\dots,N$ ), respectively.

By using the equivalent interference model [8], [32], [34], the noise is assumed to be divided into a large number,  $K$ , weak interferers, each would have equal average power  $\sigma_n^2/K$ . Therefore, the total number of interferers would be  $L = N + K$  and the new  $K$  weak interferers would be indexed by  $i = N + 1, N + 2, \dots, L$ . Assuming  $\mathbf{h}_n$  is an iid zero mean complex spherically invariant random vector with  $E[\mathbf{h}_n \mathbf{h}_n^H] = \mathbf{I}$ , while  $K \rightarrow \infty$ , the covariance matrix  $\mathbf{R}$  can be rewritten as

$$\begin{aligned} \mathbf{R} &= \sum_{i=1}^N \mathbf{A}_i \mathbf{A}_i^H + \lim_{K \rightarrow \infty} \frac{\sigma_n^2}{K} \sum_{i=N+1}^L \mathbf{h}_i \mathbf{h}_i^H \\ &= \lim_{K \rightarrow \infty} \sum_{i=1}^L \mathbf{A}_i \mathbf{A}_i^H \end{aligned} \quad (2.10)$$

If the limiting process can be handled mathematically, the equivalent interference model is exact for the system in Figure 2.7.

The adaptive array processing by means of minimum mean-squared error or optimum combining (OC) has been extensively discussed in [51]. The application of this diversity technique to wireless communication was investigated in many literatures.

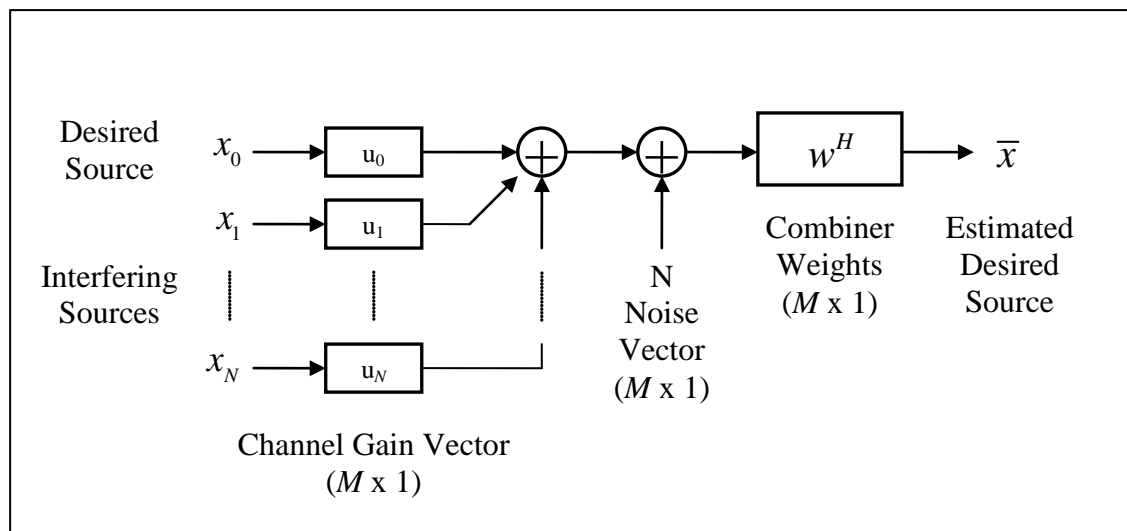


**Figure 2.7** Complex-baseband communication systems [52]

It has been known that when the adaptive antenna array at the receiver in digital cellular radio systems employs OC, the weight vector that maximize the output signal-to-interference-plus-noise ratio (SINR) is given as in [32].

$$\mathbf{w} = a \mathbf{R}^{-1} \mathbf{A}_0 \quad (2.11)$$

where  $a$  is an arbitrary constant that does not affect the SINR at the output of array. The corresponding SINR at the output of the combiner, employing the covariance matrix  $\mathbf{R}$  from the equivalent interference model in (2.11), can be written as [36]

$$\gamma = \mathbf{A}_0^H \mathbf{R}^{-1} \mathbf{A}_0 = \lim_{K \rightarrow \infty} \left\{ \mathbf{A}_0^H \left( \sum_{i=1}^L \mathbf{A}_i \mathbf{A}_i^H \right)^{-1} \mathbf{A}_0 \right\} \quad (2.12)$$

Assuming that the characteristic probability density function (pdf), corresponding to the faded interferers, are uncorrelated, i.e., all the interfering signals are modulated by the different non-negative random variable  $u_i$  ( $i = 1, 2, 3, \dots, N$ ), which is also independent of  $u_0$  that modulates the desired signal. The interferer power relative to the desired source are signified by  $\Gamma_i = P_i / P_0$  ( $i = 1, 2, 3, \dots, N$ ) and its inverse are signified by  $\Omega_i = 1 / \Gamma_i$ . By using the equivalent interference model, the cdf of the output SINR  $P_\gamma(\gamma)$ , given  $r_i$ , can be illustrated as [52]–[54]

$$P_\gamma(\gamma | r_i) = 1 - \lim_{K \rightarrow \infty} \frac{\sum_{m=0}^{M-1} \beta_m \gamma^m}{\prod_{i=1}^L \left( 1 + \frac{\gamma}{r_i \Omega_i} \right)} = 1 - \frac{\exp(-\sigma_n^2 \gamma) \sum_{m=0}^{M-1} \beta_m \gamma^m}{\prod_{i=1}^N \left( 1 + \frac{\gamma}{r_i \Omega_i} \right)} \quad (2.13)$$

where  $\beta_0 = 1$ ,  $\beta_1 = \sum_{i=1}^N \Gamma_i$ ,  $\beta_2 = \sum_{1 \leq i_1 < i_2 \leq N} \Gamma_{i_1} \Gamma_{i_2}$ ,  $\dots$ ,  $\beta_N = \Gamma_1 \Gamma_2 \dots \Gamma_N$ ,  $r_i = (u_0 / u_i)^2$  is a random variable.

The characteristic pdf of  $u_i$  in (2.7) generally utilized to form the SIRV is a jointly uncorrelated student-t distribution [55]. If it is assumed that  $u_0$  and  $u_i$  are all iid and uncorrelated, the pdf of  $r_i = (u_0 / u_i)^2$  can be obtained as in [58].

$$p_{r_i}(r_i) = \frac{\Gamma(2\alpha) r_i^{\alpha-1}}{\Gamma^2(\alpha) (1+r_i)^{2\alpha}} \quad (2.14)$$

where  $\alpha$  is the corresponding degree of freedom (DOF) of  $u_0$  and  $u_i$ , and  $\Gamma$  is a Gamma function. The student-t distribution typically becomes a Gaussian distribution (Rayleigh) as  $\alpha \rightarrow \infty$ .

## 2.5 System Model

Generally, in mobile radio communication systems, the channel experience multipath fading and the performance of the system degraded due to CCI. We consider a wireless communication system with  $M$ -element array output consists of desired signal,  $L$  interfering signals, and thermal noise may be written as.

$$\mathbf{R} = \mathbf{u}_0 \mathbf{u}_0^H + \sum_{i=1}^L \mathbf{u}_i \mathbf{u}_i^H + \sigma^2 \mathbf{I} \quad (2.15)$$

where  $x_0(t)$  and  $\{x_1(t), x_2(t), \dots, x_i(t)\}$  are transmitted data sequence and set of interfering source, respectively. Each source comes from some independent identically distributed zero mean random process.  $\mathbf{u}_0, \mathbf{u}_1, \mathbf{u}_2, \dots, \mathbf{u}_i$  are the corresponding  $M \times 1$  vectors.  $\mathbf{n}$  is an  $M \times 1$  additive noise vector. Each noise source in this vector is an independent zero mean complex Gaussian process with magnitude variance  $\sigma^2$ .

The SIRP model is to be useful to characterize the fading channel statistic, and then we assume further that each component of the vectors  $\mathbf{u}_i$  follows a complex spherically invariant random vector (SIRV) [53]. We model  $\mathbf{u}_i$  as a positive-valued SIRP distribution satisfying

$$\mathbf{u}_i = r_i \mathbf{Z}_i \quad (2.16)$$

where  $\mathbf{Z}_i$  is Rayleigh distributed with mean power of  $P_0$  and  $P_i$  ( $i = 1, 2, 3, \dots, N$ ), respectively and  $r_i$  is any positive valued random variable having a pdf  $f_r(r)$ . The exact distribution of the output SINR of an idealized linear MMSE diversity combiner operating in a Rayleigh fading additive interference channel was derived in [53]. The maximum SINR at the output combiner corresponding to MMSE can be written as

$$\gamma = \mathbf{u}_0^H \mathbf{R}^{-1} \mathbf{u}_0 \quad (2.17)$$

The output SINR,  $\gamma$  can be shown to be given by

$$\gamma = \mathbf{u}_0^H \left[ \sum_{i=1}^L r_i \mathbf{u}_i \mathbf{u}_i^H + a \mathbf{I} \right]^{-1} \mathbf{u}_0, \quad (2.18)$$

where  $r_i = (u_0 / u_i)^2$ ,  $a = \sigma^2 / u_0^2$  and  $\sigma^2$  is the magnitude variance of the thermal noise vector  $\mathbf{n}$ . To evaluate the system performance, the equivalent interference model [55] is applied. The reliability function can be written as [53]-[55]

$$f(\gamma | r_i) = 1 - \frac{\exp(-\sigma_n^2 \gamma) \sum_{i=0}^{M-1} D_i \gamma^i}{\prod_{i=1}^L (1 + \Gamma_i \gamma / r_i)} \quad (2.19)$$

where the interferer powers relative to desired source are denote by  $\Gamma_i = P_i / P_0$ , ( $i = 1, 2, 3, \dots, L$ ) and  $D_i$  is the coefficient of  $\gamma^i$  in  $\prod_{i=1}^L (1 + \Gamma_i \gamma)$  . i.e.,

$$D_i = \sum_{1 \leq n_1 < \dots < n_i \leq L} \Gamma_{n_1} \Gamma_{n_2} \dots \Gamma_{n_i}$$

is a random variable defined in [53].

The following MIMO single-user Gaussian channel is considered, with  $t$  antennas at the transmitter and  $r$  antennas at the receiver

$$\mathbf{y} = \mathbf{H}\mathbf{x} + \mathbf{n} \quad (2.20)$$

$\mathbf{H}$  is the  $r \times t$  channel matrix with i.i.d. entries  $h_{ij}$ , each distributed as the random variable  $Z$  defined as  $z = \text{Re}^{j\theta}$ . The vector  $\mathbf{y} \in C^r$ ,  $\mathbf{x} \in C^t$ , and  $\mathbf{n}$  is zero-mean complex Gaussian noise with  $\mathbf{E}[\mathbf{x}^\dagger \mathbf{x}] = \mathbf{I}$ . In addition, a total transmit power constraint  $\mathbf{E}[\mathbf{x}^\dagger \mathbf{x}] \leq P$  is assumed. For a given input covariance matrix  $\Sigma$ , the MIMO instantaneous capacity is given by

$$C(\Sigma) = \log_2 \det(\mathbf{I} + \mathbf{H}\Sigma\mathbf{H}^\dagger) \quad (2.21)$$

And the MIMO channel capacity therefore given by

$$C = \log_2 \det\left(\mathbf{I} + \frac{P}{t} \mathbf{W}\right) \quad (2.22)$$

where

$$\mathbf{W} = \begin{cases} \mathbf{H}\mathbf{H}^\dagger & r \leq t \\ \mathbf{H}^\dagger \mathbf{H} & r > t \end{cases} \quad (2.23)$$

The channel exhibits multiple inputs and multiple outputs and its capacity can be estimated by the extended Shannon's capacity formula, as described below.

We consider an antenna array with  $n_t$  elements at the transmitter and an antenna array with  $n_r$  elements at the receiver. The impulse response of the channel between the  $j$ th transmitter element and the  $i$ th receiver element is denoted as  $h_{i,j}(\tau, t)$ . The MIMO channel can then be described by the  $n_r \times n_t$   $\mathbf{H}_{i,j}(\tau, t)$  matrix:

$$\mathbf{H}_{i,j}(\tau, t) = \begin{bmatrix} h_{1,1}(\tau, t) & h_{1,2}(\tau, t) & \cdots & h_{1,n_t}(\tau, t) \\ h_{2,1}(\tau, t) & h_{2,2}(\tau, t) & \cdots & h_{2,n_t}(\tau, t) \\ \vdots & \vdots & \ddots & \vdots \\ h_{n_r,1}(\tau, t) & h_{n_r,2}(\tau, t) & \cdots & h_{n_r,n_t}(\tau, t) \end{bmatrix} \quad (2.24)$$

The matrix elements are complex numbers that correspond to the attenuation and phase shift that the wireless channel introduces to the signal reaching the receiver with delay  $\tau$ . The input-output notation of the MIMO system can now be expressed by the following equation:

$$\mathbf{y}(t) = \mathbf{H}(\tau) \otimes \mathbf{s}(t) + \mathbf{u}(t) \quad (2.25)$$

where  $\otimes$  denotes convolution,  $\mathbf{s}(t)$  is a  $n_t \times 1$  vector corresponding to the  $n_t$  transmitted signals,  $\mathbf{y}(t)$  is a  $n_r \times 1$  vector corresponding to the  $n_r$  received signals and  $\mathbf{u}(t)$  is the additive white noise.

If we assume that the transmitted signal bandwidth is narrow enough that the channel response can be treated as flat across frequency, then the discrete time description corresponding to (2.25) is

$$\mathbf{r}_\tau = \mathbf{H}\mathbf{s}_\tau + \mathbf{u}_\tau \quad (2.26)$$

Under these assumptions, using the capacity expression in the limit of finite number of sub-channels, it allows to achieve the Shannon capacity in fragmented primary user spectrum. i.e.

$$C = \int_{\Omega} \frac{1}{2} \log_2 \left[ 1 + \frac{G(f)S_0}{N_0} \right] df \quad (2.27)$$

where  $\Omega$  is the collection of unused spectrum segments,  $G(f)$  is the channel power gain at frequency  $f$ ,  $S_0$  and  $N_0$  are the signal and noise power per unit frequency respectively.

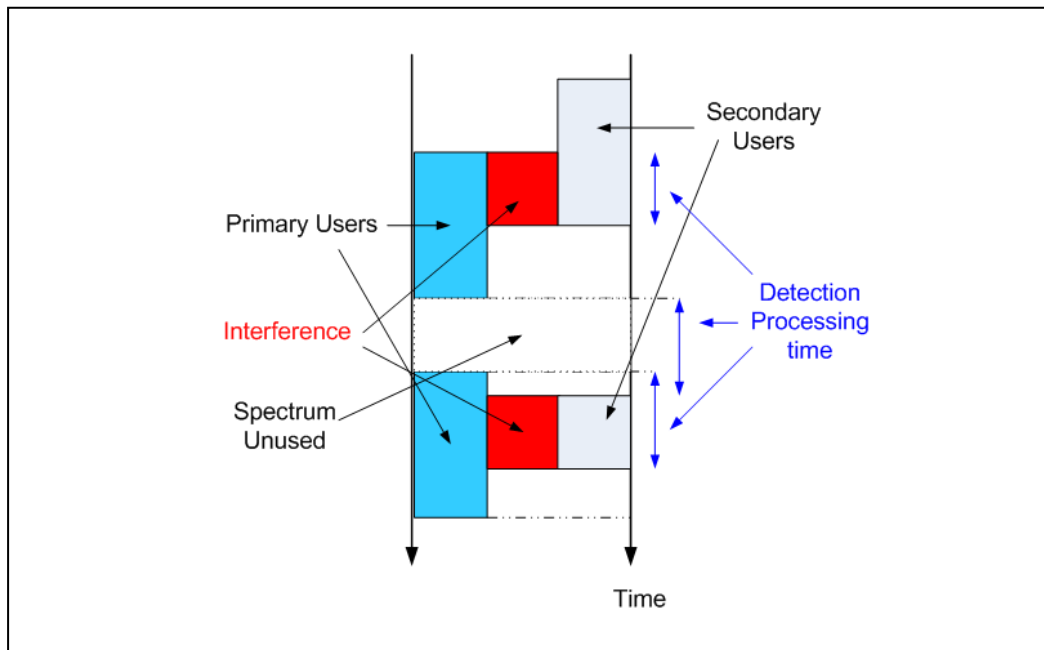


**Figure 2.8** An example of problems that detection delays

It is the key that will enable flexible, efficient and reliable spectrum use by dynamically sensing the radio's operating characteristics to the real-time. Smart radios have the potential to utilize the large amount of unused spectrum in an intelligent way while no harmful interference user of the spectrum. Figure 2.7 shows an example of detection delay, secondary user cause interference to licensed user. In a spectrum hole is defined as a frequency band that is assigned to a licensed user exclusively, but that is not allocated by this user at a specific time and place. Spectrum can be classified into three types that indicate the amount of interference in a specific band, the spaces are partially occupied by local interferers called *black spaces*. The spaces are partially occupied is *grey spaces* and if spaces are empty of local interferers is known as *white spaces* or spectrum holes.